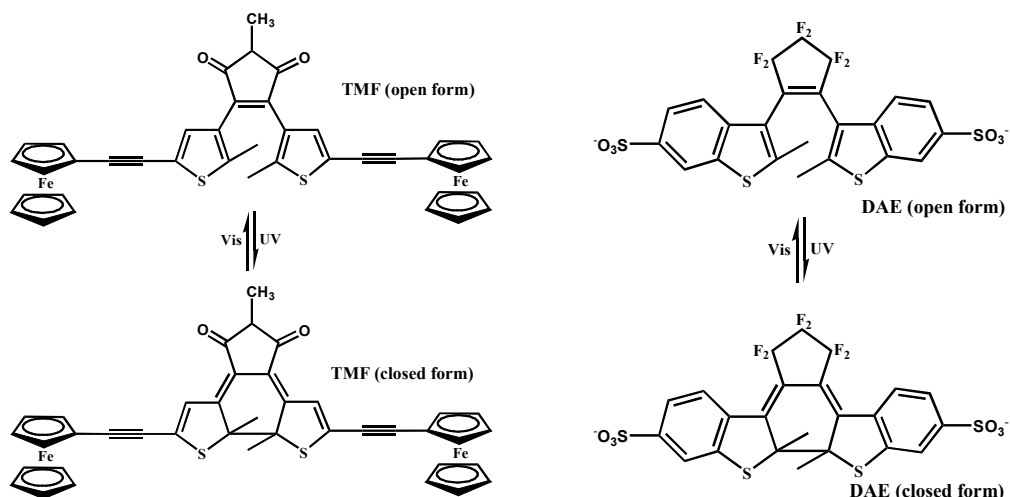
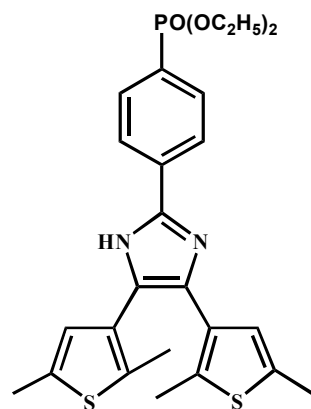


Electronic Supporting Information



Scheme S1



Scheme S2

Table S1 Solid-state emission data of **1**, **1L**, and **dbi** at room temperature

| Compound | λ_{\max} (nm) |
|------------|-------------------------|
| 1 | 423, 452, 484, 518, 570 |
| 1L | 437, 459, 482, 522, 565 |
| dbi | 423 |

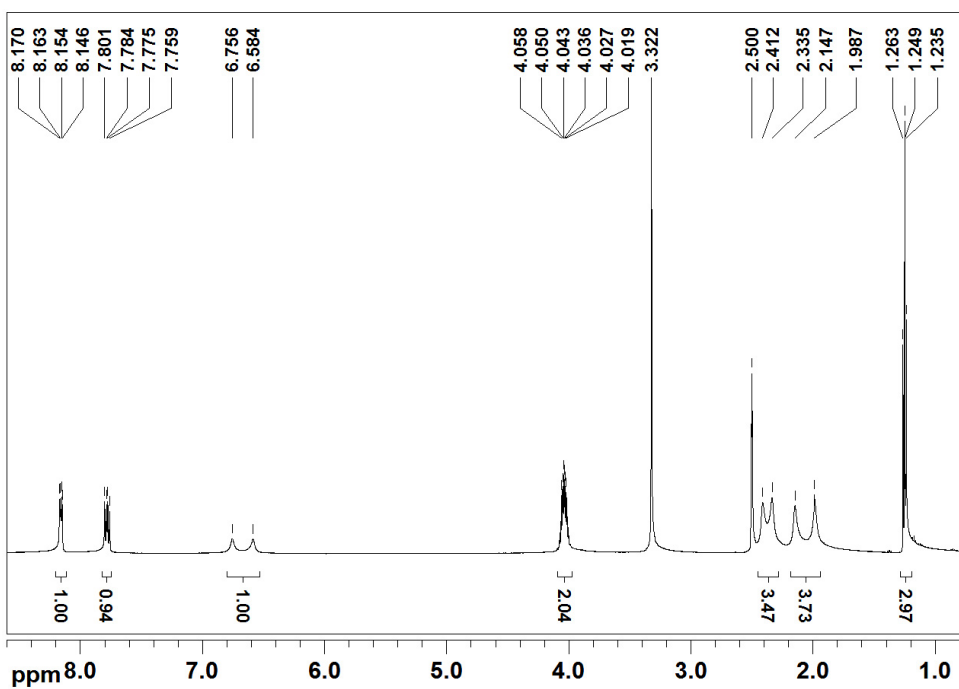


Fig. S1 ¹H NMR spectrum of dbi before irradiation with 365 nm light (500 MHz, DMSO-*d*₆).

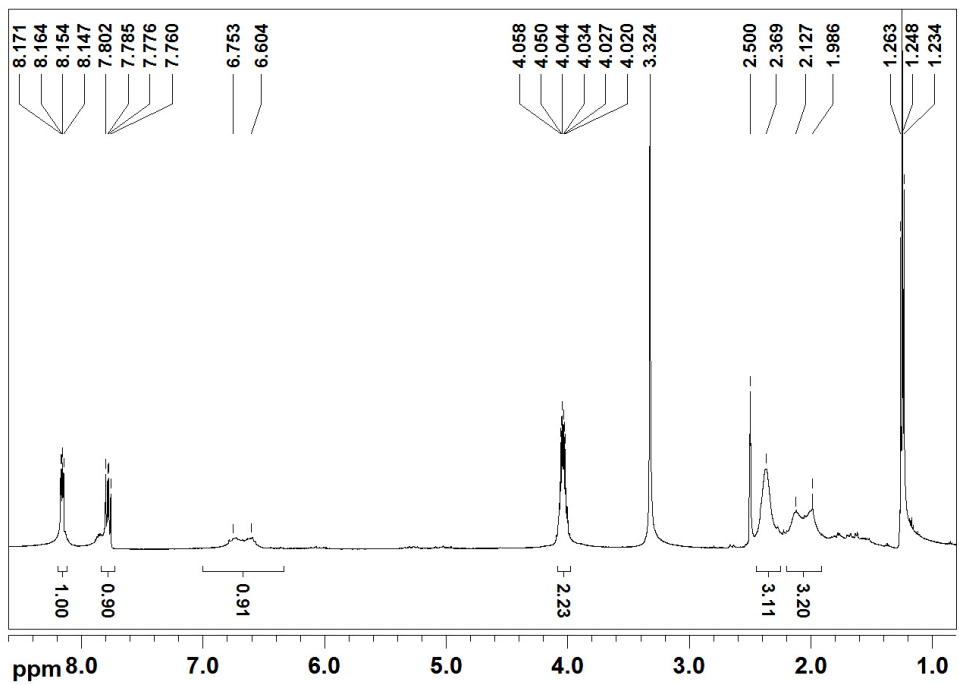


Fig. S2 ¹H NMR spectrum of dbi after irradiation with 365 nm light (500 MHz, DMSO-*d*₆).

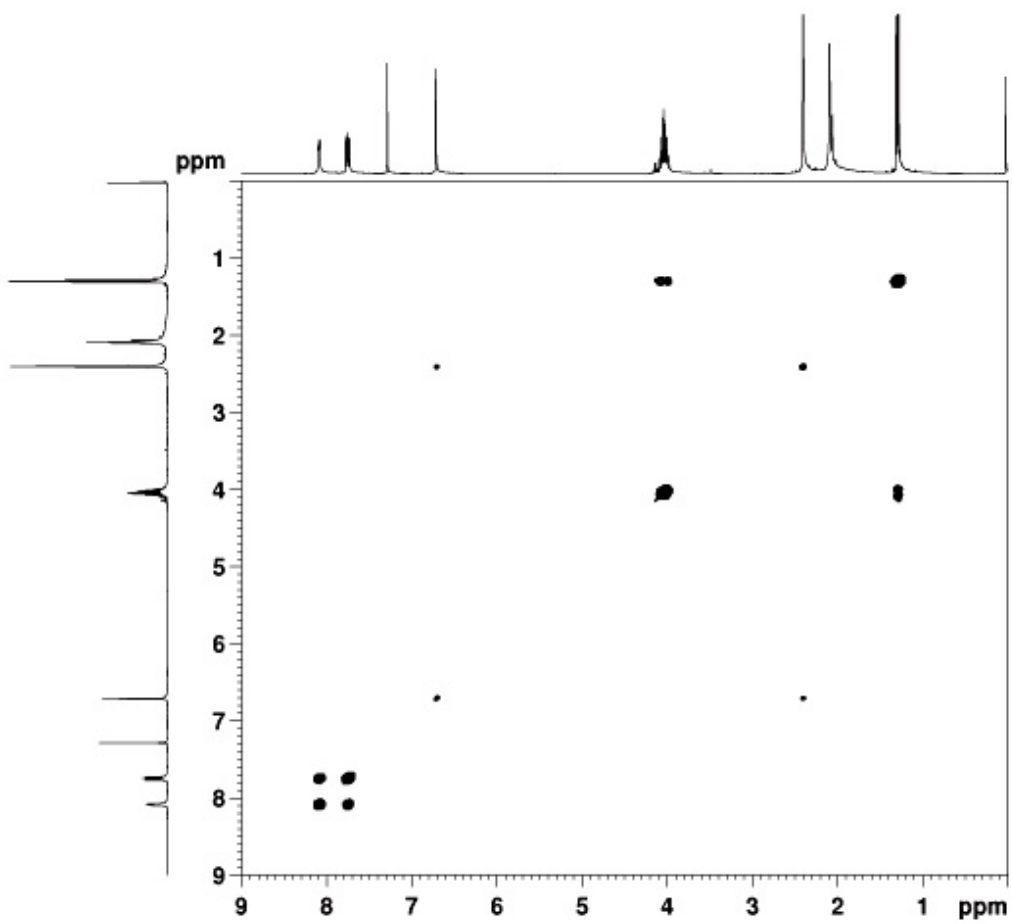


Fig. S3 COSY NMR spectrum of dbi (500 MHz, CDCl_3).

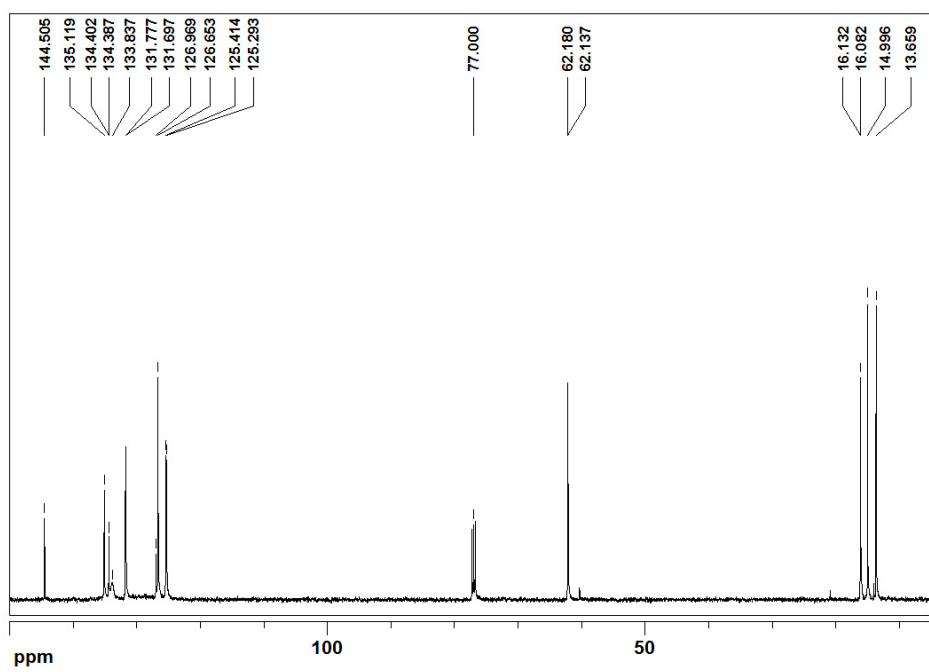


Fig. S4 ^{13}C NMR spectrum of dbi (500 MHz, CDCl_3).

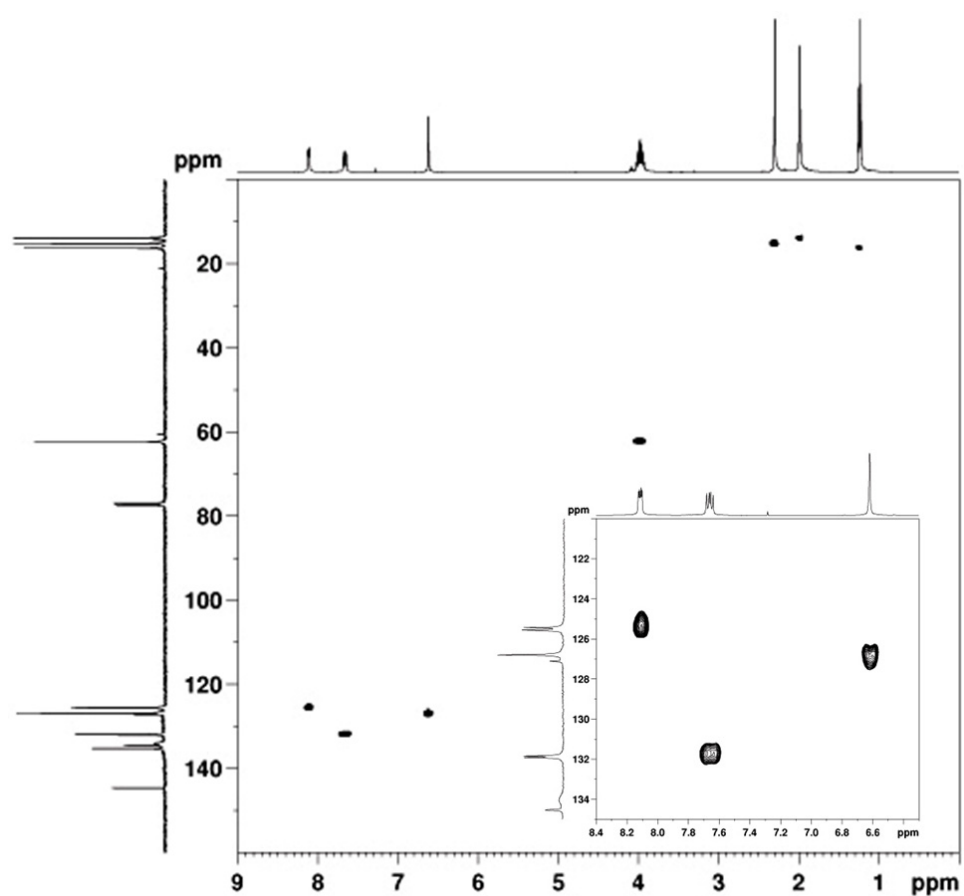


Fig. S5 HSQC NMR spectrum of dbi (500 MHz, CDCl_3). Inset: ^{13}C signals in 120–135 ppm.

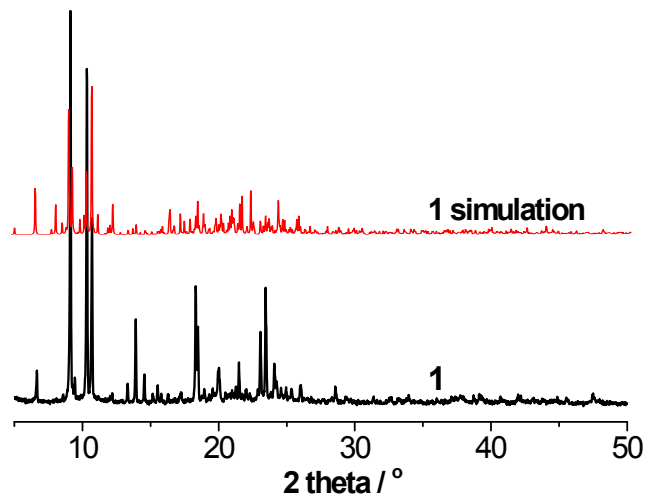


Fig. S6 Experimental and simulated XRD patterns of **1**.

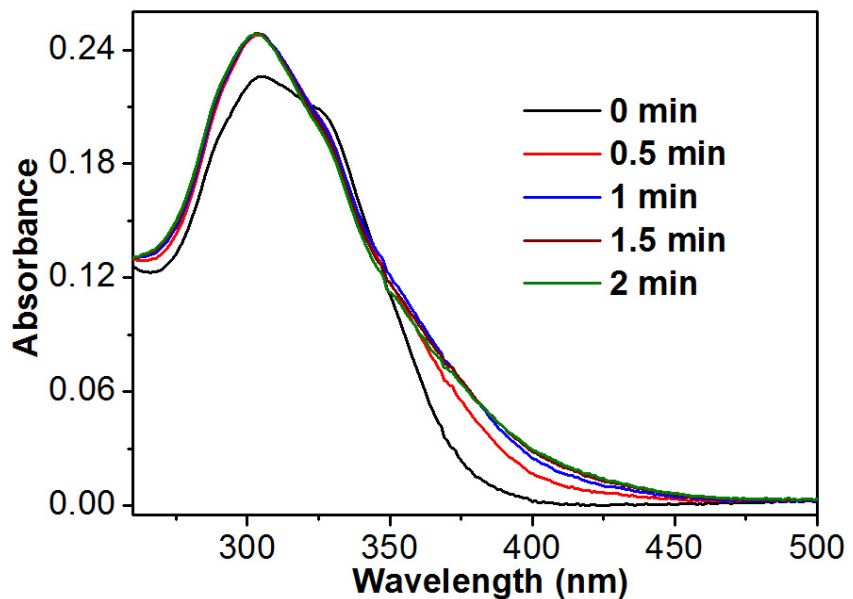


Fig. S7 Absorption-spectra of **1** in CH_3CN solution ($c = 1.1 \times 10^{-5} \text{ M}$) upon UV irradiation ($\lambda = 365 \text{ nm}$) for 0 - 2 minutes.

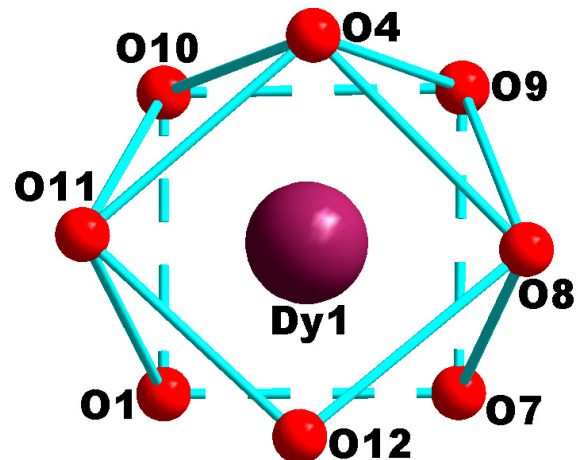


Fig. S8 The coordination geometry of Dy(III) ion in **1**.

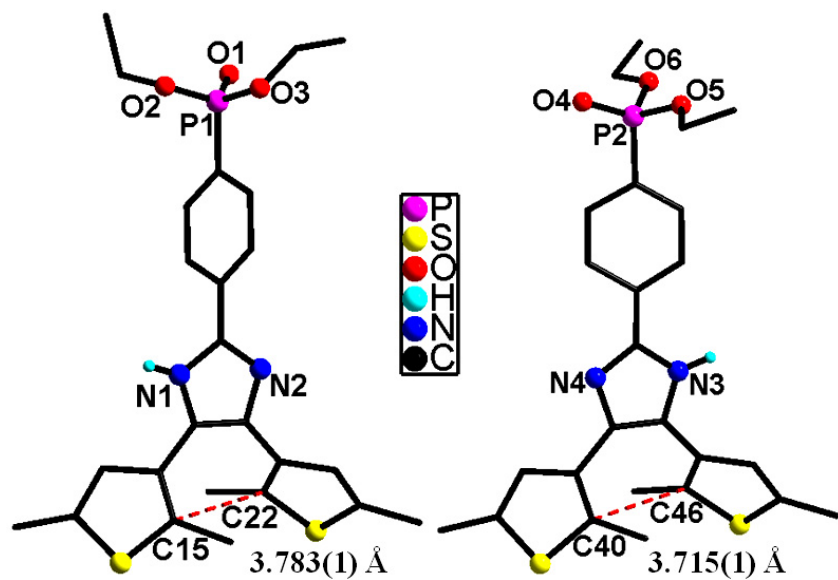


Fig. S9 Antiparallel conformations of dbi ligands in **1**. All H atoms attached to C atoms are omitted for clarity.

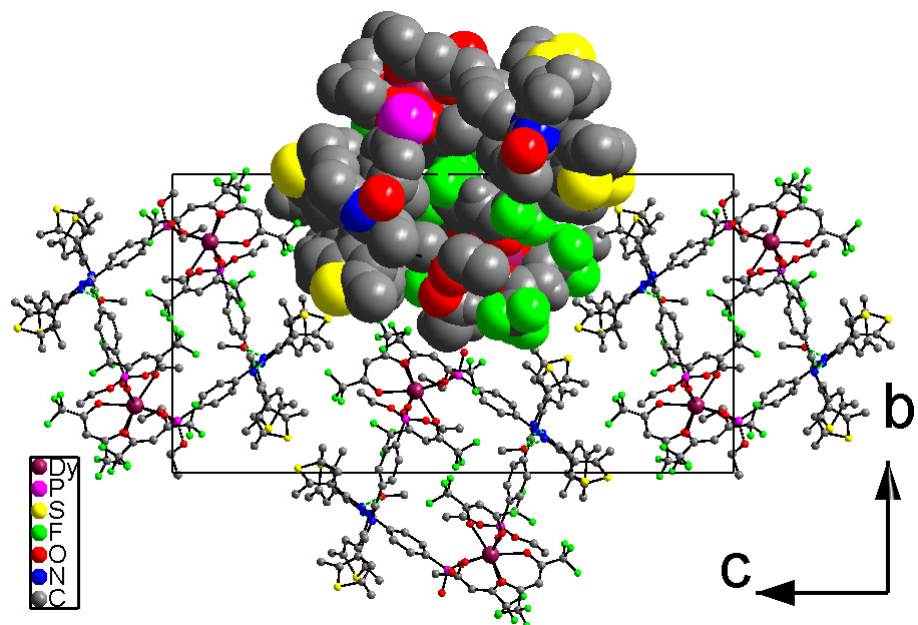


Fig. S10 The packing structure of **1**.

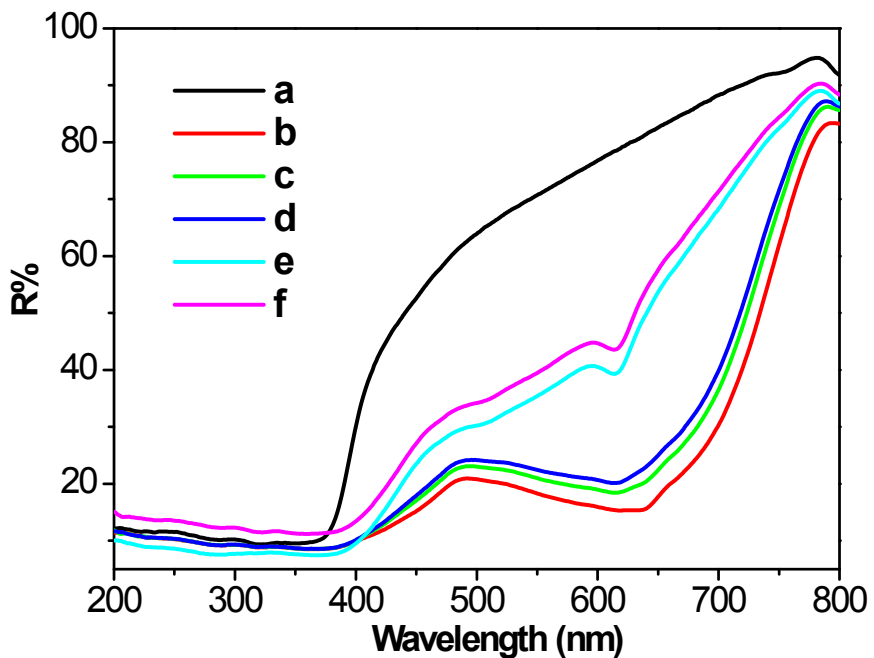


Fig. S11 Plots a and b: irradiating ($\lambda = 365$ nm) dbi for 0, 20 minutes, respectively; plots c and d: placing the sample corresponding to plot b in the dark for 15, 30 minutes, respectively; plots e and f: irradiating ($\lambda = 580$ nm) the sample corresponding to plot b for 1 and 2 minutes, respectively.

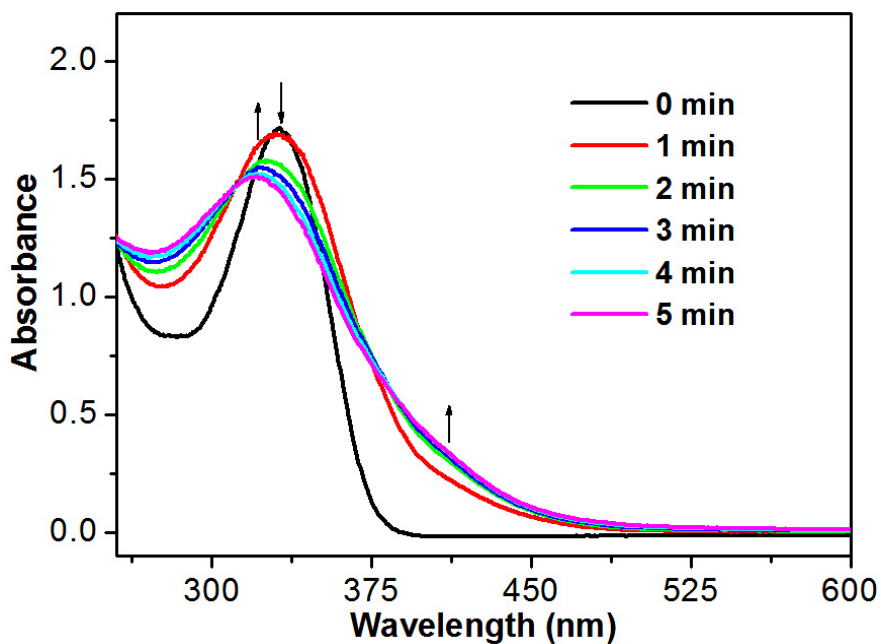


Fig. S12 Absorption-spectra changes of dbi in CH_3CN solution ($c = 2.0 \times 10^{-5}$ M) upon UV irradiation ($\lambda = 365$ nm) for 0 - 5 minutes.

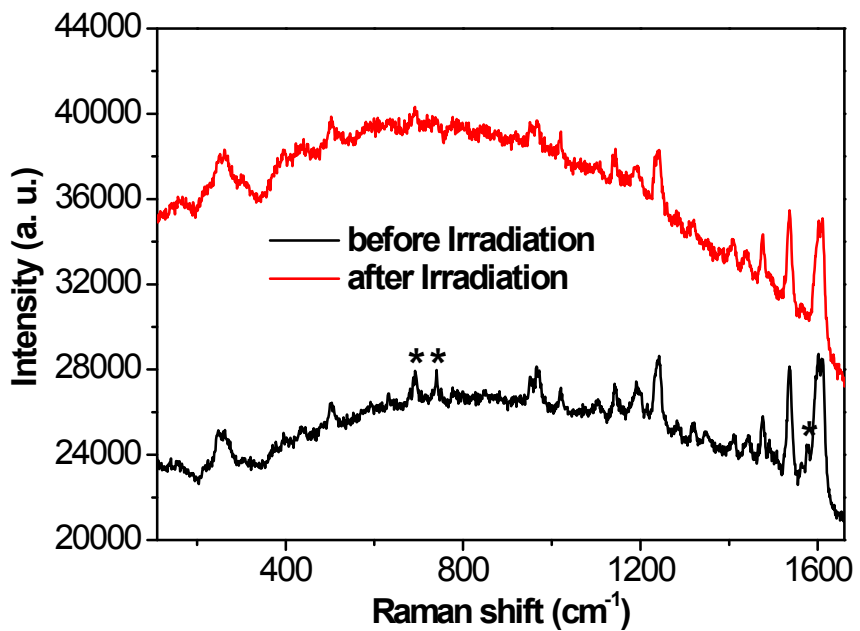


Fig. S13 Raman spectra of **1** before and after irradiation ($\lambda = 365$ nm, 20 minutes), using laser light of 785 nm. Three peaks with * are at 691, 740 and 1575 cm⁻¹, respectively.

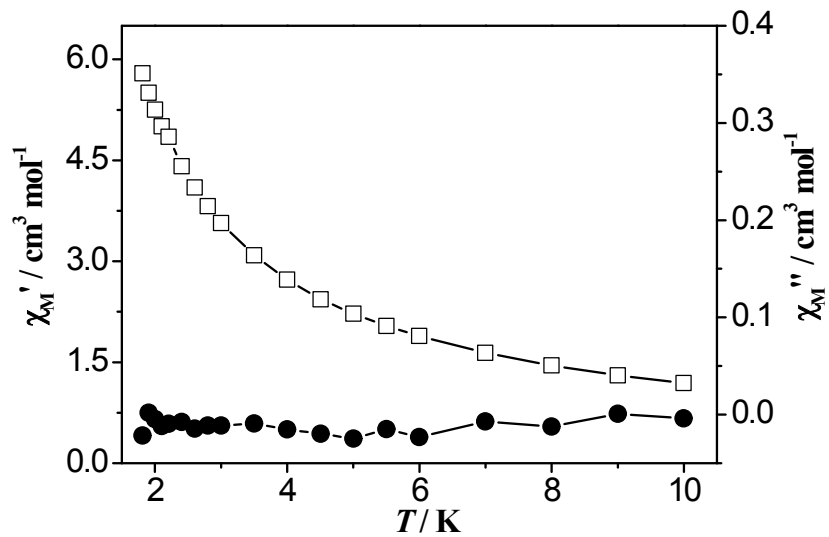


Fig. S14 Temperature-dependent ac susceptibilities of in-phase χ_M' and out-of-phase χ_M'' for **1** under zero static field with a frequency of 1488 Hz in the temperature range of 1.8-10 K.

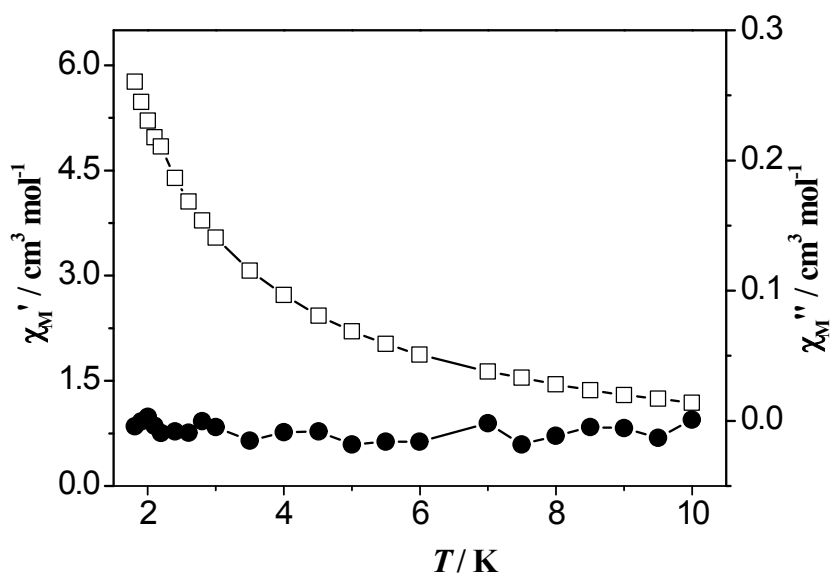


Fig. S15 Temperature-dependent ac susceptibilities of in-phase χ_M' and out-of-phase χ_M'' for **1L** under zero static field with a frequency of 1488 Hz in the temperature range of 1.8-10 K.

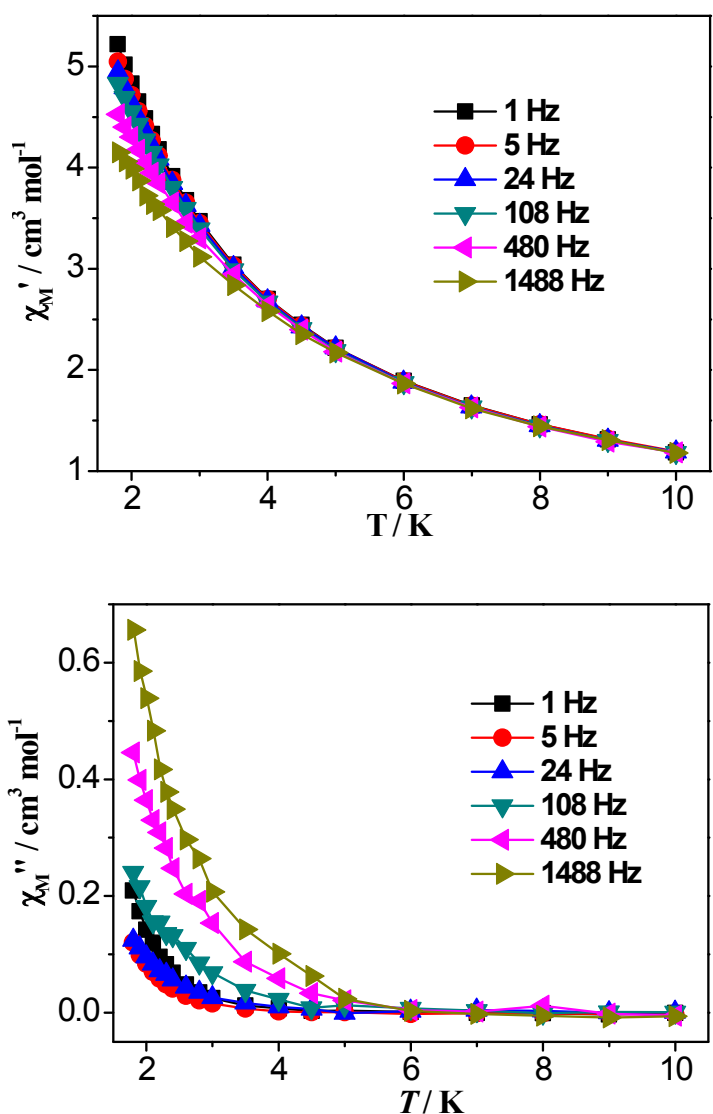


Fig. S16 Temperature-dependent ac susceptibilities of in-phase χ_M' (top) and out-of-phase χ_M'' (bottom) for **1** with $H_{dc} = 1000$ Oe and $H_{ac} = 5$ Oe.

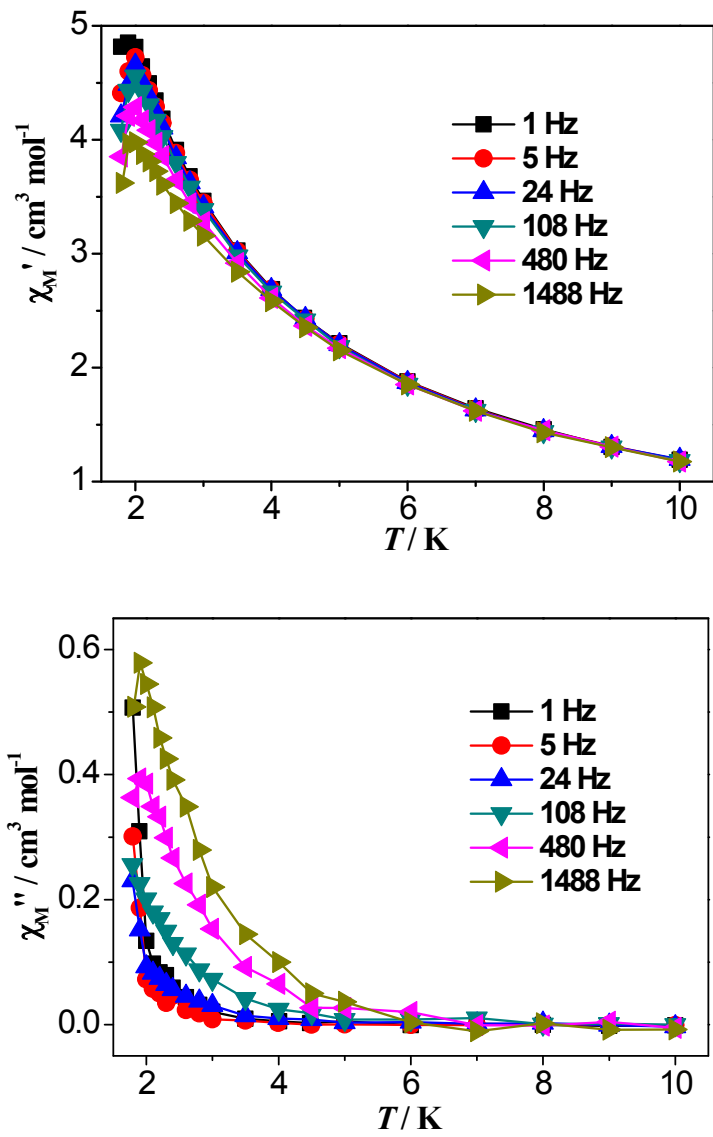


Fig. S17 Temperature-dependent ac susceptibilities of in-phase χ_M' (top) and out-of-phase χ_M'' (bottom) for **1L** with $H_{dc} = 1000$ Oe and $H_{ac} = 5$ Oe.

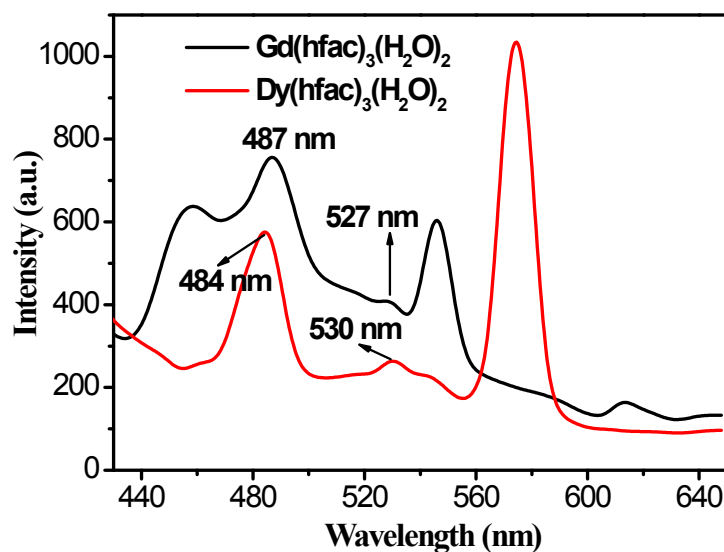


Fig. S18 Solid-state emission spectra for $\text{Gd}(\text{hfac})_3(\text{H}_2\text{O})_2$ and $\text{Dy}(\text{hfac})_3(\text{H}_2\text{O})_2$ under $\lambda_{\text{ex}} = 370 \text{ nm}$ at room temperature.